Neurobiology of Disease 58 (2013) 183–190

Contents lists available at SciVerse ScienceDirect

Neurobiology of Disease

journal homepage: www.elsevier.com/locate/ynbdi

Divergent α-synuclein solubility and aggregation properties in G2019S LRRK2 Parkinson's disease brains with Lewy Body pathology compared to idiopathic cases☆

Adamantios Mamais [a,b], Meera Raja [a,b], Claudia Manzoni [b], Sybille Dihanich [b], Andrew Lees [a,b], Darren Moore [c], Patrick A. Lewis [b,d], Rina Bandopadhyay [a,b,*]

[a] Reta Lila Weston Institute of Neurological Studies UCL Institute of Neurology, 1, Wakefield Street, WC1N 1PJ, UK
[b] Department of Molecular Neuroscience, UCL Institute of Neurology, Queen Square, London WC1N 3BJ UK
[c] Ecole Polytechnique Federale de Lausanne (EPFL), Brain and Mind Institute, School of Life Sciences, 1015 Lausanne, Switzerland
[d] School of Pharmacy, University of Reading, Whiteknights, Reading, RG6 6AP, UK

ARTICLE INFO

Article history:
Received 12 December 2012
Revised 18 April 2013
Accepted 22 May 2013
Available online 5 June 2013

Keywords:
LRRK2
G2019S
α-Synuclein
Differential solubility
Immunohistochemistry

ABSTRACT

Mutations in LRRK2 are the most common genetic cause of Parkinson's disease (PD). The most prevalent LRRK2 mutation is the G2019S coding change, located in the kinase domain of this complex multi-domain protein. The majority of G2019S autopsy cases feature typical Lewy Body pathology with a clinical phenotype almost indistinguishable from idiopathic PD (iPD). Here we have investigated the biochemical characteristics of α-synuclein in G2019S LRRK2 PD post-mortem material, in comparison to pathology-matched iPD. Immunohistochemistry with pS129 α-synuclein antibody showed that the medulla is heavily affected with pathology in G2019S PD whilst the basal ganglia (BG), limbic and frontal cortical regions demonstrated comparable pathology scores between G2019S PD and iPD. Significantly lower levels of the highly aggregated α-synuclein species in urea–SDS fractions were observed in G2019S cases compared to iPD in the BG and limbic cortex. Our data, albeit from a small number of cases, highlight a difference in the biochemical properties of aggregated α-synuclein in G2019S linked PD compared to iPD, despite a similar histopathological presentation. This divergence in solubility is most notable in the basal ganglia, a region that is affected preclinically and is damaged before overt dopaminergic cell death.

Introduction

Mutations in the LRRK2 gene, first identified in 2004 (Paisan-Ruiz et al., 2004; Zimprich et al., 2004), are one of the most common genetic causes of PD (Tan and Skipper, 2007). Recent genome wide association studies have also identified LRRK2 as a risk locus for idiopathic PD (iPD) (Nalls et al., 2011), highlighting this gene as one of the key genetic factors in the aetiopathogenesis of PD. LRRK2 codes for a large multidomain protein harbouring several putative protein–protein interaction motifs, along with a GTPase and a kinase domain (Mata et al., 2006). Mutations that segregate with disease are restricted to the enzymatic core of the protein, suggesting that the kinase and GTPase activities of LRRK2 are linked to this protein's role in PD (Ross et al., 2011). The G2019S mutation lies in the kinase domain and is the most common cause of autosomal dominant PD, accounting for up to 2% of all PD cases (Martin et al., 2010). Patients harbouring LRRK2 mutations manifest clinical features almost indistinguishable from the idiopathic form of the disease (Healy et al., 2008). The neuropathology associated with LRRK2 mutations, however, is variable and encompasses α-synuclein positive Lewy bodies (LBs), tau positive inclusions, TDP-43 aggregates, ubiquitin only inclusions and pure nigral cell loss with no inclusions (Wider et al., 2010). Nonetheless, nigral cell loss is the common pathological feature amongst all of the LRRK2 mutation cases, with the majority of cases (including those with the G2019S mutation) displaying α-synuclein positive pathology (Cookson et al., 2008; Poulopoulos et al., 2012).

The G2019S mutation is thought to increase LRRK2 kinase activity, as documented by augmented autophosphorylation and phosphorylation of other generic targets (Greggio and Cookson, 2009; Greggio et al., 2006; Smith et al., 2005; Smith et al., 2006; West et al., 2005). The pleomorphic pathology associated with the G2019S mutation suggests that LRRK2 may act upstream of α-synuclein, tau and TDP-43, underlining the need to identify signalling pathways linked

* Corresponding author at: Reta Lila Weston Institute of Neurological Studies UCL Institute of Neurology, 1, Wakefield Street, WC1N 1PJ, UK.
E-mail address: rina.bandopadhyay@ucl.ac.uk (R. Bandopadhyay).

Available online on ScienceDirect (www.sciencedirect.com).

0969-9961/$ – see front matter © 2013 The Authors. Published by Elsevier Inc. All rights reserved.
http://dx.doi.org/10.1016/j.nbd.2013.05.017

to LRRK2. A wide range of putative phosphorylation targets and interacting proteins for LRRK2 have been proposed, including α-synuclein, 4E-BP1, moesin, tubulin, dvl, lrp6 and ArfGAP1 (Berwick and Harvey, 2012; Gandhi et al., 2008; Imai et al., 2008; Jaleel et al., 2007; Qing et al., 2009; Sancho et al., 2009; Stafa et al., 2012). The physiological relevance of the majority of these interactions are yet to be determined whilst some may have limited implications *in vivo* (Trancikova et al., 2012). In transgenic mice, an interaction between LRRK2 and α-synuclein has been suggested by Lin et al. (2009) who demonstrated that the presence of excess WT/G2019S LRRK2 can accelerate the progression of A53T α-synuclein mediated neuropathology in a CAMKII driven inducible model, and promote the formation of high molecular weight α-synuclein aggregates — with ablation of LRRK2 acting to modulate pathology. Intriguingly, this study reported a decrease in phosphorylation of α-synuclein upon over-expression of the G2019S mutation. In contrast, further studies using the hind-brain selective prion protein promoter to drive LRRK2 expression failed to detect an effect on α-synuclein pathology in A53T transgenic mice, and thus not supporting a pathophysiological interaction *in vivo* whilst high LRRK2 levels improved motor skills in a mouse model and was insufficient to drive neuronal α-synucleinopathy (Daher et al., 2012; Herzig et al., 2012; Lin et al., 2009). Interestingly, however, accumulation of α-synuclein monomers and high molecular weight species along with development of α-synuclein inclusions have been reported in the kidneys of LRRK2 KO mice with age (Tong et al., 2009).

Further genetic evidence that LRRK2 and *SNCA* (the gene coding for α-synuclein) are linked comes from a recent study demonstrating that a polymorphism in *SNCA* is associated with lower age of onset for LRRK2 patients (Botta-Orfila et al., 2012). Furthermore, a current study has shown lower levels of α-synuclein in leukocytes of patients with G2019S LRRK2 mutation (Pchelina et al., 2011) and that α-synuclein and LRRK2 may be expressed synergistically in rodents (Westerlund et al., 2008). In addition, our group has shown that α-synuclein pathology affected regions in iPD and G2019S PD express lower levels of LRRK2 transcript compared to controls, in the absence of an effect on global gene expression levels (Devine et al., 2011; Sharma et al., 2011). However, the nature of the interaction between LRRK2 and α-synuclein, two of the most important autosomal dominant players in genetic Parkinson's, remains ambiguous.

At the Queen Square Brain Bank, we hold four G2019S cases that have α-synuclein positive LB pathology. We sought to explore the pathological and biochemical characteristics of α-synuclein in the presence of this mutation in LRRK2. The aim of this study was to investigate the morphological distribution and solubility of α-synuclein in the G2019S cases compared to iPD cases, matched for pathology, and control cases. We show that, despite extensive LB pathology, highly aggregated α-synuclein species are largely absent in the G2019S PD cases examined.

Methods

Case details and tissue collection

Post-mortem human brain tissues from 14 cases were obtained from the Queen Square Brain Bank collection and one G2019S case was obtained from the Sun Health Research Institute, USA. Appropriate consent was obtained in all cases and approval for this study was granted by the local Research Ethics Committee. The 4 G2019S PD cases in our brain bank were classified neuropathologically (by consultant neuropathologists) as the limbic sub-type for α-synuclein pathology according to McKeith consensus criteria (McKeith et al., 2005). The 5th G2019S case, from Sun Health, also harboured the limbic subtype of α-synuclein pathology. The routine α-synuclein immunohistochemistry is done using pre-treatment with formic acid (10 min) and pressure cooking in citrate buffer at pH 6.0 to expose antigenic sites. The primary antibody used is against α-synuclein (Novocastra) at a dilution of 1:75. The iPD cases chosen were pathology matched, whilst the controls had no signs of any significant neuropathology and did not suffer from any neurological disease. Clinical phenotype of the G2019S and iPD cohorts were that of slow progressive parkinsonism with good levodopa response. Flash frozen tissue was obtained from the basal ganglia (caudate and putamen), limbic (entorhinal cortex) cortex and frontal cortex of these cases (care was taken to dissect the correct anatomical regions for biochemical analysis). Immunohistochemistry (IH) on formalin fixed sections for phospho-α-synuclein was performed on sections of medulla, substantia nigra, basal ganglia, entorhinal cortex, cingulate gyrus and frontal cortex where available. Restricted demographics of the cases are presented in Table 1.

Immunohistochemistry

Immunohistochemistry (IH) was performed on formalin fixed paraffin embedded 8 μm sections from a number of regions namely, medulla, substantia nigra, basal ganglia, entorhinal cortex, cingulate gyrus, and frontal cortex from four G2019S, four iPD and four control cases as listed in Table 2. The cases and controls were stained at the same time. Sections were dewaxed, and quenched for endogenous peroxidase activity using methanol and 0.3% H_2O_2. The sections were pre-treated with proteinase K (Dako) for 15 min to expose antigenic sites. Following thorough washes, non-specific binding on sections was blocked for 1 h with 10% non-fat milk in 1× PBS. The sections were then incubated with anti-phospho-Ser129-α-synuclein (Monoclonal, a kind gift of Dr John Anderson, Elan Pharmaceuticals) 1: 2000 for 1 h at room temperature. Following thorough washes, the sections were sequentially incubated with biotinylated secondary antibody (anti-mouse, Vector Laboratories) at 1:200, followed by treatment with avidin-biotin peroxidase complex (ABC, Vector Laboratories) for 30 min each. Following a series of washes in 1× PBS, IH was visualised using hydrogen peroxide-activated diaminobenzidine (Sigma). The sections were then dehydrated in graded ethanol (70–100%) followed by xylene and then mounted in DPX (VWR). The pS129 antibody has been extensively characterised for immunoblots and immunohistochemistry (Anderson et al., 2006; Guerreiro et al., 2012).

Phospho-α-synuclein scores

The severity of pS129 α-synuclein scores was assessed independently by two researchers based on a 3 point scoring system at ×20 objective. Score: where + corresponds to 1 LB, sparse Lewy neurites (LNs) and dot like structures, score ++ was given when the number

Table 1
Selective demographic data of cases studied. PMD: post-mortem delay (h).

Case	Sex	Age (yrs)	PMD (h)	pH	Disease duration (yrs)	α-Synuclein pathology
G2019S 1	F	80	44.4	6	28	Limbic
G2019S 2	F	81	15	6.53	16	Limbic
G2019S 3	F	84	32.2	5.79	N/A	Limbic
G2019S 4	F	72	24.55	6.1	15	Limbic
G2019S 5 (FCx)	M	85	1.66	N/A	11	Limbic
iPD 1	F	69	52.5	6.2	14	Limbic
iPD 2	M	70	61.2	6.29	12	Limbic
iPD 3	F	87	47.45	6.62	13	Limbic
iPD 4	M	75	48	6.0	17	Limbic
iPD 5	F	88	11.3	6.38	10	Limbic
Control 1	F	85	37	6.4	–	–
Control 2	M	93	112	5.86	–	–
Control 3	F	91	98.5	6.26	–	–
Control 4	M	87	36	6.1	–	–
Control 5	F	68	41.5	5.98	–	–

Table 2
Immunohistochemistry scores for phosphorylated α-synuclein depositions in the various regions studied. Severity of pS129 α-synuclein positive pathology from different regions of G2019S and idiopathic PD cases was scored by two researchers independently on a three point scoring system where "+", "++", "+++" indicate mild, moderate and severe pathologies respectively. N/A indicates section not available for staining. DMN = dorsal motor nucleus of the vagus.

Case	DMN	Midbrain	Striatum	Entorhinal cortex	Cingulate gyrus	Frontal cortex
G2019S 1	+++	+++	+++	+++	N/A	+
G2029S 2	+++	+++	++	N/A	N/A	+
G2019S 3	+++	++	+++	++	+	+
G2019S 4	N/A	++	++	+++	+	+
iPD 1	++	+++	++	+++	+	+
iPD 2	++	+++	++	+++	+	+
iPD 3	+++	+++	++	++	+	+
iPD 4	++	++	+++	++	+	+

of lesions corresponded to between 2–10 LBs and the presence of mild numbers of neurites, +++ score was given when the number of LBs were greater than 10 and also containing numerous LNs and dot like structures. Independent data scores were compared and consensus results derived.

Differential ultracentifugation and fractionation

10% (w/v) homogenates were prepared from 1 g tissue from the basal ganglia, limbic cortex and frontal cortex regions in homogenisation buffer [20 mM Tris–HCl pH 7.4, 150 mM NaCl, 1× protease inhibitor cocktail (EDTA free; ROCHE) and 1× phosphatase inhibitor cocktail (ROCHE)] with the aid of a mechanical homogeniser, and cleared by centrifugation at 1000 *g* for 5 min at 4 °C. The supernatant was designated as cleared homogenate. The cleared homogenates were centrifuged at 100,000 *g* for 1 h at 4 °C and the supernatant was labelled as the TBS-soluble fraction. The pellet was washed twice with homogenisation buffer, resuspended in 2.5 ml homogenisation buffer with 5% (w/v) SDS, sonicated (5 × 20 s) and centrifuged at 100,000 *g* for 30 min at 16 °C. The supernatant was designated as the SDS-soluble fraction. The pellet was rinsed twice with homogenisation buffer with 5% (w/v) SDS and re-suspended by sonication in 50 μl homogenisation buffer containing 8% (w/v) SDS and 8 M urea, sonicated and designated as the urea-soluble fraction. The protein concentrations were calculated by BCA protein assay (Pierce).

Western blotting

30 μg (for cleared homogenates, TBS and SDS soluble fractions) and 6 μg (for the urea-soluble fractions) of each sample were analysed by immunoblot using 12% polyacrylamide gels (BIO-RAD). After transfer to PVDF membranes they were blocked in PBS, 0.1% Tween X-100, 5% BSA and an antibody against α-synuclein (BD Transduction Laboratories) was used at 1:750 dilution in overnight incubation at 4 °C in PBS, 0.1% Tween X-100, 1% BSA. Secondary HRP-conjugated antibody (Santa Cruz) was used at 1:2000 dilution for 1 h at room temperature. For the dot-blot, 3 μg of the urea-soluble fractions were blotted on activated PVDF membrane and were left to air-dry, followed by a standard western blot processing. For the western blots the bands were quantitated using the NIH ImageJ software and the graphs and statistics were generated in GraphPad Prism. The band intensities were normalised to an internal control for comparison across groups and subsequently expressed as relative ratios of the monomeric synuclein over the β-actin. The statistical tests used were Mann–Whitney *U* test, ANOVA (Bonferroni correction) and ANCOVA as indicated in the text.

Results

Phospho-S129 α-synuclein pathology in G2019S and idiopathic PD

The iPD cases chosen from the QSBB archive were matched for α-synuclein pathology with the G2019S LRRK2 mutation cases and all were classified as having limbic sub-type distribution according to the McKeith criteria for classification of LBs (McKeith et al., 2005). The α-synuclein pathology for three of our G2019S cases has been discussed briefly by Gilks et al. (2005).

Immunohistochemical analysis of pS129 α-synuclein revealed staining for LBs and LNs in sites of LB predilection namely medulla, substantia nigra, basal ganglia, entorhinal cortex and frontal cortex in both the G2019S and iPD (Fig. 1). The pS129 α-synuclein immunohistochemistry was semi-quantitatively assessed for severity of pathology in the G2019S and idiopathic PD. Data are summarised in Table 2. The scoring pattern is consistent with the cases fulfilling the criteria for limbic sub-type for α-synuclein pathology with higher scores noted in the amygdala and entorhinal cortex and only few LBs were noted in the frontal cortex. The pS129 α-synuclein antibody stained typical LBs, small and large neurites, whilst also several dot-like positive structures were noted in the neuropil of all of the regions examined. It is noteworthy that 3 G2019S cases where medulla sections were available had severe pathology in the dorsal motor nucleus of the vagus (DMN). The control cases used in this study had no pS129 α-synuclein positive inclusions (Fig. 1).

α-Synuclein solubility in G2019S brains

The levels and solubility of the monomeric α-synuclein species were investigated in basal ganglia, limbic cortex and frontal cortex tissue from G2019S, iPD and control brains. Cleared homogenates were prepared from the tissues followed by fractionation to produce TBS-soluble, SDS-soluble and urea-soluble fractions. A trend towards an increase in monomeric α-synuclein was observed across the PD spectrum compared to controls in basal ganglia cleared homogenates, with the G2019S being significantly higher than controls in the limbic cortex (Figs. 2A, B, C) ($p < 0.05$; Mann–Whitney *U* test). In both TBS-soluble and SDS-soluble fractions, higher levels of monomeric α-synuclein were observed in iPD versus controls in the basal ganglia, which reflects and follows the similar trend observed in basal ganglia homogenates (Figs. 2D, G) (for basal ganglia TBS iPD: control, $p < 0.05$; Mann–Whitney *U*). The G2019S also showed higher TBS-soluble α-synuclein compared to controls but the G2019S SDS-soluble levels did not follow the trend of the iPD cases, rather they were comparable to the controls (for TBS G2019S: controls, $p < 0.05$; Mann–Whitney *U*) (Figs. 2D, G). These effects in the distribution of monomeric α-synuclein species across soluble fractions were largely minimised in the frontal cortex, which is not affected by Lewy Body pathology (Figs. 2F, I).

The most significant observation on a possible effect of a mutant LRRK2 genotype on α-synuclein biochemistry came from looking at the urea-soluble fractions of these cases, which represent highly insoluble species that are insoluble in 5% SDS containing buffer. In the urea-soluble fractions, detection of α-synuclein was largely absent in the G2019S and control cases whilst highly aggregated α-synuclein species were detected in the majority of the iPD samples from the basal ganglia and the limbic cortex (Figs. 3A, B). The single band detected in the G2019S urea-soluble fractions was indicative of monomeric α-synuclein running between the 14 kDa and 19 kDa protein standards. To address the possibility that the α-synuclein species in the urea-fraction of G2019S are in fact insoluble in urea and therefore not separated by SDS-PAGE, a dot-blot experiment was performed where equal amounts of urea-soluble fractions were blotted and probed for α-synuclein (Fig. 3C). This indicated significantly lower levels of α-synuclein species in the urea-fraction of

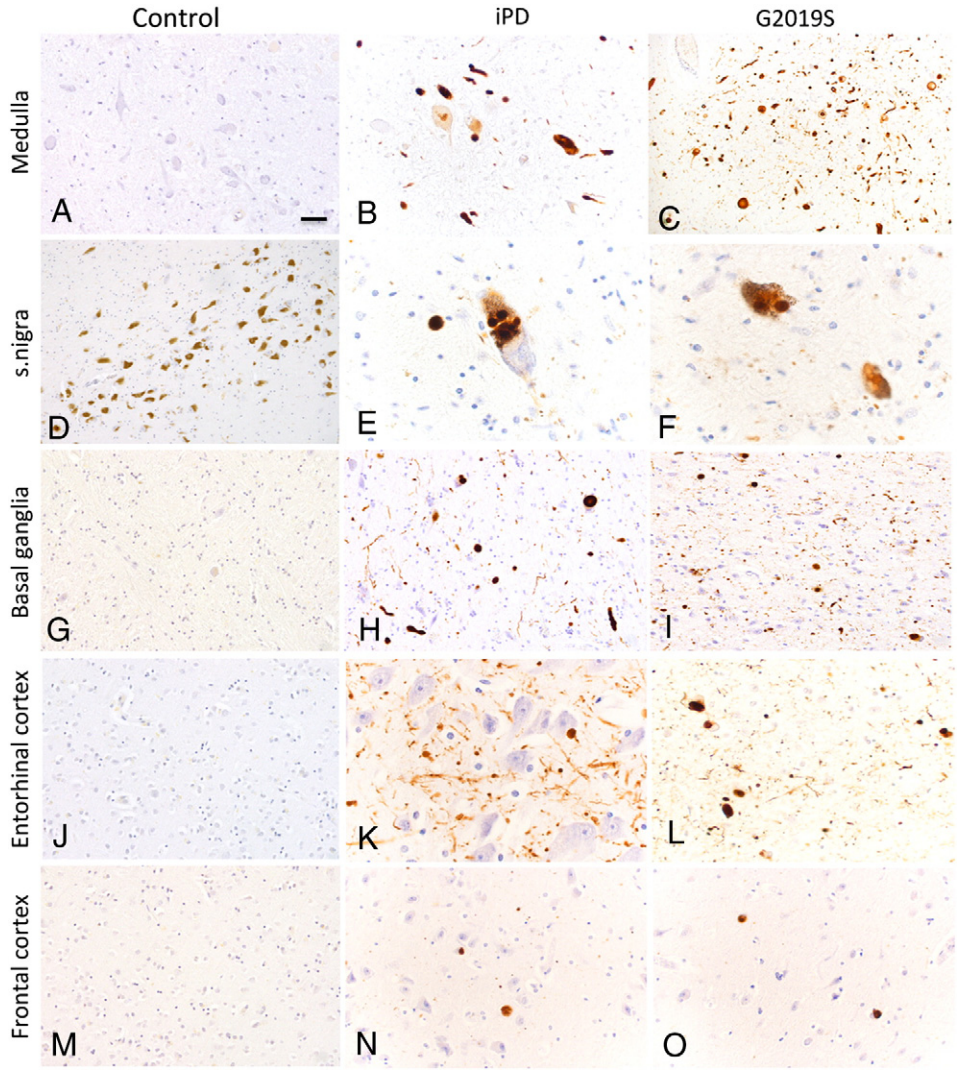

Fig. 1. Immunohistochemistry of pS129 α-synuclein inclusions in G2019S, iPD and control post-mortem brains. Formalin fixed sections were stained for pS129 α-synuclein. All of our G2019S cases are categorised as the limbic subtype of α-synuclein pathology, according to the McKeith criteria (McKeith et al., 2005). The regions examined were medulla, substantia nigra, basal ganglia (putamen), entorhinal cortex and frontal cortex. The DMN (dorsal motor nucleus of vagus) of the G2019S cases tended to have higher pS129 α-synuclein inclusions whilst comparable pS129 α-synuclein staining is observed in inclusion bodies in G2019S and idiopathic PD in the nigra, limbic cortex and frontal cortex. Scale bar correspond to10 μm in A, B, E, F, H, K, and L and 20 μm in C, D, G, I, J, M, N, and O.

G2019S compared to iPD, whilst the controls did not show any detectable positivity for the protein.

The G2019S and iPD cases had comparable post-mortem delays (PMDs) whilst the controls showed a wider spread of values but not statistically significant divergence (Fig. S2A). A possible effect of PMD on protein stability that could skew the results obtained by the urea-soluble fractions was investigated by analysis of covariance. Adding PMD as the covariate on the urea-soluble α-synuclein data showed that the G2019S cases have statistically significant lower α-synuclein levels compared to the iPD group even after controlling for a possible effect of PMD (ANCOVA; basal ganglia: $F_{2,10} = 19.37$, $p < 0.001$; limbic cortex: $F_{2,10} = 17.12$, $p = 0.001$). In fact, a linear regression plot of the urea-soluble data for iPD over PMD further suggests that the levels of α-synuclein in this fraction do not covary with PMD (Fig. S2E). Linear regression analyses of monomeric α-synuclein levels over PMD were performed for all data to investigate a possible effect of PMD on the levels of α-synuclein across the different fractions. As depicted in Fig. S2B, there is a slight trend of negative correlation in the α-synuclein levels in homogenates over PMD, but this is not significant ($r^2 = 0.041$, $p = 0.54$). Similar results were obtained from the SDS and TBS soluble data, revealing non-significant correlation to PMD (Figs. S2C, D).

Discussion

The most important finding of this study is the divergent solubility properties observed for α-synuclein in G2019S PD post-mortem brains compared to iPD cases, despite a similar distribution of α-synuclein pathology. Significantly, differential ultracentifugation followed by immunoblot analysis revealed that α-synuclein species were largely absent in the urea soluble fraction in G2019S PD. To our knowledge, this is the first detailed study comparing solubility of α-synuclein in LRRK2 G2019S and pathology matched idiopathic PD cases as an attempt to directly dissect the nature of the LRRK2-synuclein interplay in post-mortem familial PD tissue.

A key factor facilitating this study is that the iPD cohort has been carefully matched to the G2019S cases in terms of pathology progression and severity, namely the limbic subtype according to McKeith et al. (2005), and this allows us to interpret any differences seen in α-synuclein biochemistry between these two series as a consequence of LRRK2 aberrant function. The tissue used in the biochemical analysis was dissected from precise regions of the caudate and putamen, entorhinal and frontal cortex in all the cases and in matching topology with the sections used in histological analysis from the formalin-fixed side of the donated brain, to minimise possible variability in LB pathology.

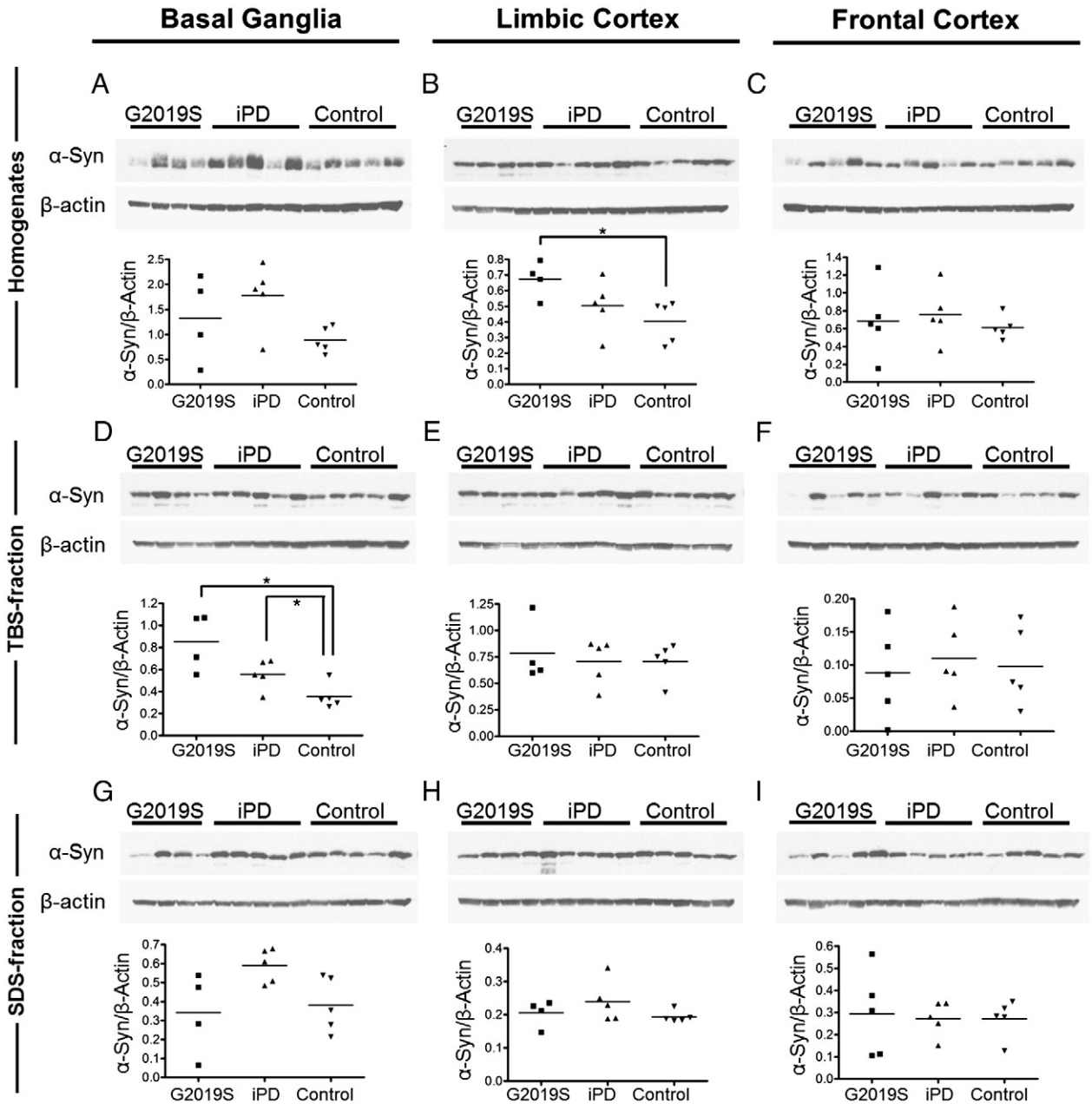

Fig. 2. Distribution of α-synuclein monomer across cleared homogenates, TBS and SDS soluble fractions of G2019S, iPD and control post-mortem brain. The levels of α-synuclein in cleared homogenates (A, B, C), TBS (D, E, F) and SDS (G, H, I) soluble fractions of three G2019S, iPD and control brain regions were examined. A trend of increased solubility of α-synuclein in G2019S compared to that in iPD is observed in basal ganglia (D, G), that is not evident in the less pathologically affected areas of the cortex (E, F, H, I). [Mann–Whitney *U* test: $^{*}p < 0.05$].

By immunohistochemistry we demonstrate an abundance of pS129 α-synuclein in LBs and LNs in all the disease cases in sites of LB predilection. This is consistent with earlier data examining iPD cases (Anderson et al., 2006; Fujiwara et al., 2002). We also demonstrate abundant pS129 α-synuclein pathology in the medulla, a region that is affected early in disease (Braak et al., 2003; Kingsbury et al., 2010) suggesting that phosphorylation of α-synuclein is an early event in disease pathogenesis and might be involved in disease propagation (Kondo et al., 2011; Li et al., 2008). The DMN of the G2019S cases were more severely affected compared to the iPD cohort. The limbic cortex (entorhinal cortex) displayed substantial pS129 α-synuclein pathology in all the PD cases examined, whilst fairly mild involvement of the frontal cortex was apparent in these cases (Fig. 1; Table 2). These results are consistent with the G2019S and iPD cases being of the limbic category for α-synuclein pathology. The pS129 α-synuclein dot-like pathology observed in the neuropil in the disease cases is likely to represent synaptic pathology (Muntane et al., 2008). The α-synuclein antibodies used in this study have been previously characterised for immunohistochemistry and immunoblots (Anderson et al., 2006; Guerreiro et al., 2012; Miller et al., 2004). As previously described, the pS129 α-synuclein antibody necessitated the use of proteinase-K to reveal antigenic sites. Consequently, our control cases were devoid of any pS129 α-synuclein immunoreactivity.

We used brain tissue from the basal ganglia, limbic cortex (entorhinal cortex) and frontal cortex to generate cleared homogenates followed by serial fractionation into TBS, SDS and urea-soluble fractions and investigated the distribution of α-synuclein across these

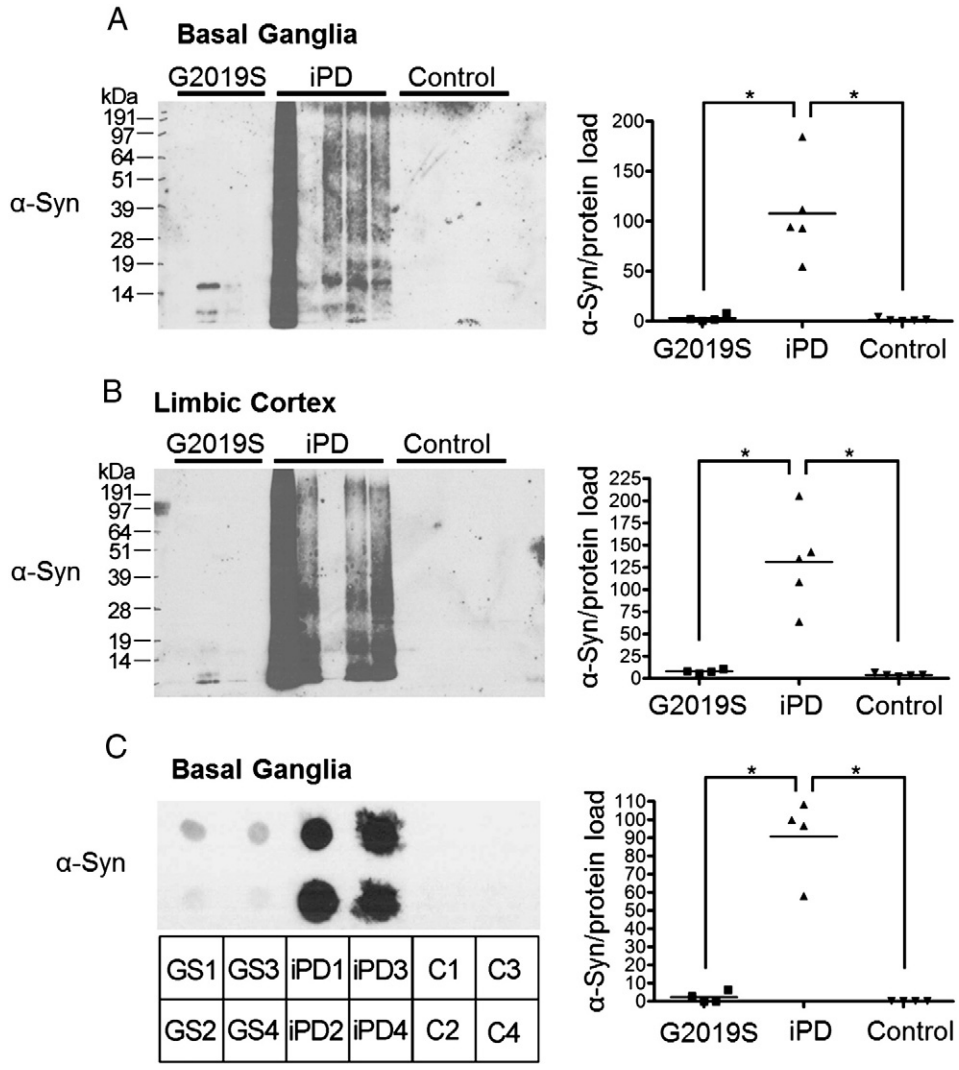

Fig. 3. Divergence of G2019S PD brains in levels of highly aggregated urea-soluble α-synuclein species. The urea-soluble fractions of basal ganglia (A) and limbic cortex (B) of G2019S, iPD and control brains were analysed for the presence of α-synuclein. Aggregated α-synuclein is observed in the basal ganglia and the limbic cortex of the iPD samples following pathology severity. Very little aggregated synuclein is detected in the urea-soluble samples of the G2019S cases compared to the iPD cases. A dot-blot of urea-fractions of the basal ganglia (C) reveals much lower levels of α-synuclein in the G2019S cases compared to that of the iPD samples, whilst no α-synuclein is detected in controls. [ANOVA with Bonferroni's correction: $^{*}p < 0.01$].

fractions. Aggregated α-synuclein is the principal component of LBs in PD (Spillantini et al., 1997). A number of studies have described high levels of pS129 α-synuclein species in LBs, suggesting a link to the pathological process — a notion further supported by the increased phosphorylation at Ser129 residue reported in A53T transgenic mice (Anderson et al., 2006; Campbell et al., 2000; Fujiwara et al., 2002; Wakamatsu et al., 2007). Along with hyperphosphorylation, LB disease accompanies accumulation of significantly higher levels of SDS-soluble and SDS-insoluble α-synuclein species compared to control brain (Campbell et al., 2000; Zhou et al., 2011). Our data suggests that G2019S PD may diverge from this model. We report the absence of detectable α-synuclein species in the urea fraction (SDS insoluble) of the basal ganglia and limbic cortex of G2019S PD cases (Figs. 3A, B). This is further verified by dot-blot data that exclude the presence of α-synuclein species that would be insoluble in urea and therefore not be separated and detected by SDS-PAGE (Fig. 3C). In addition we observe a trend of higher TBS-soluble levels of monomeric α-synuclein compared to controls perhaps reflecting an increase in cytosolic α-synuclein, along with no increase in the membrane-enriched SDS-soluble fraction in the basal ganglia of the G2019S samples (Figs. 2D, G). Nevertheless we detect comparably abundant higher molecular weight α-synuclein species in G2019S and iPD cleared homogenates from the basal ganglia (Fig. S1A), suggesting that the differences seen in the fractions may in fact be an effect of differential solubility properties of α-synuclein.

An important caveat of this study is that the substantia nigra, the most relevant region to study the consequences of dopamine cell loss, was not available from our G2019S mutation cases. The regions studied herein are those that survived the dopaminergic system neurodegeneration and therefore may not directly inform us as to the pathogenic pathways involved in the substantia nigra, nonetheless these regions are associated with the rostrocaudal propagation of α-synuclein disease pathology (Braak et al., 2003) and some may be afflicted pre-clinically (Booij and Knol, 2007). We show extensive α-synuclein synaptic and neuritic pathology in both G2019S and iPD cases suggestive of synaptic degeneration (Muntane et al., 2008). The basal ganglia have a functional link to the substantia nigra playing a crucial role in modulating the activity of dopaminergic neurons (Lee and Tepper, 2009). Furthermore, it has also been suggested that dopaminergic neurodegeneration can be a result of α-synuclein aggregate-related synaptic dysfunction through a dying back phenomenon initiated in the basal ganglia (Schulz-Schaeffer, 2010).

This could highlight how the divergent biochemical properties of pathogenic α-synuclein in the basal ganglia of G2019S PD could in fact drive a different progression pathway to that of iPD.

The fact that the iPD and G2019S cases share comparable LB pathology makes this divergence in α-synuclein biochemistry an intriguing finding. A previous report suggested that the biochemical abnormalities of α-synuclein protein might not be related with the presence of LBs in G2019S PD cortical regions (Gomez and Ferrer, 2010). Interestingly, in the PD-related movement disorder multiple system atrophy, which is characterised by α-synuclein inclusions in oligodendrocytes, studies have observed no SDS-insoluble α-synuclein species (Campbell et al., 2001) whilst Galvin et al. reported a case of NB1A with α-synuclein inclusions where highly insoluble α-synuclein oligomeric species were absent, although the protein was detected in the SDS soluble fraction (Galvin et al, 2000). It has also been reported that the metabolomic profile of G2019S LRRK2 mutants has a unique biochemical signature (Johansen et al., 2009) further reinforcing the hypothesis that some aspects of the pathomechanisms underlying PD may vary between genetic and idiopathic causes (Johansen et al., 2011). A recent study described a molecular interaction between LRRK2 and α-synuclein in both endogenous and overexpression conditions, along with an effect of LRRK2 levels on α-synuclein pathology, indicating that the interaction between the two proteins can indeed be very complex (Guerreiro et al., 2012).

The precise nature of the pathogenic α-synuclein species is a matter of some debate (Cookson, 2009), however multiple lines of enquiry suggest that some forms of aggregated, oligomeric species are responsible for the cell loss associated with α-synuclein accumulation (Vekrellis et al., 2011). A recent *in vitro* study has proposed that proteinase-K-resistant oligomers that bridge the conversion of the initially formed protein oligomers to fibril formation are the disease causing forms (Cremades et al., 2012), whilst proteinase-K resistant species of S129 phosphorylated α-synuclein residue are seen in DLBs (Neumann et al., 2002). A parallel scenario may be plausible for α-synuclein in G2019S cases where the inclusions may represent benign protective inclusions similar to that seen in Huntington's disease (Arrasate et al., 2004). Thus, further studies of a proteinase-K-resistant oligomeric species may throw important light in the case of G2019S PD.

In summary, our data suggest that significantly low amounts of insoluble α-synuclein in G2019S LRRK2 could be a distinguishing feature compared to iPD. This is seen despite comparable LB pathology in both the PD groups. The fractionation experiments performed here did not specifically analyse α-synuclein deposited in LBs, but rather all α-synuclein species available to be solubilised by the extraction techniques. In this respect, solubility studies along with electron microscopy of α-synuclein isolated directly from LBs would shed light on whether the divergent solubility observed in this study is a reflection of altered global α-synuclein or specific to aggregated protein localised to Lewy bodies.

The major caveat to this study is the limited number of G2019S PD post-mortem human brain material included, a reflection of the low numbers of genetically defined post-mortem brains available to the scientific community. The data from the cleared homogenates, TBS and SDS fractions show some variability between the samples of the PD or control cases, and this reflects the limited statistical power that four G2019S cases can allow for. One the other hand, the urea fractions presented here, representing the major divergence we see for the G2019S PD cohort compared to iPD, exhibit a robust and uniform change in α-synuclein solubility, indicating a strong and reproducible difference in the biochemical properties of α-synuclein. Although brain tissue from G2019S mutation cases is rare, further replications from other cases are essential in order to fully understand the link between LRRK2 mutations and α-synuclein inclusions. In particular, examining whether this divergence in solubility holds true for mutations other than the G2019S, such as the R1441C, R1441G or Y1699C mutations, will be critical in understanding the pathogenic role of different LRRK2 mutations in neurodegeneration.

Supplementary data to this article can be found online at http://dx.doi.org/10.1016/j.nbd.2013.05.017.

Acknowledgments

We thank the neuropathologists at QSBB, Prof Tamas Revesz and Dr Janice Holton, for neuropathological diagnosis of the cases used. This study was funded by grants from the Michael J. Fox Foundation for Parkinson's Research LRRK2 consortium to R.B., P.A.L and D.M. P.A.L. is a Parkinson's UK research fellow (grant F1002). R.B. is funded by the Reta Lila Weston Trust. C.M. is funded by the Rosetrees Trust. This work was supported in part by the Wellcome Trust/MRC Joint Call in Neurodegeneration award (WT089698) to the UK Parkinson's Disease Consortium (UKPDC) whose members are from the UCL Institute of Neurology, the University of Sheffield and the MRC Protein Phosphorylation Unit at the University of Dundee.

References

Anderson, J.P., et al., 2006. Phosphorylation of Ser-129 is the dominant pathological modification of alpha-synuclein in familial and sporadic Lewy body disease. J. Biol. Chem. 281, 29739–29752.
Arrasate, M., et al., 2004. Inclusion body formation reduces levels of mutant huntingtin and the risk of neuronal death. Nature 431, 805–810.
Berwick, D.C., Harvey, K., 2012. LRRK2 functions as a Wnt signaling scaffold, bridging cytosolic proteins and membrane-localized LRP6. Hum. Mol. Genet. 21, 4966–4979.
Booij, J., Knol, R.J., 2007. SPECT imaging of the dopaminergic system in (premotor) Parkinson's disease. Parkinsonism Relat. Disord. 13, S425–S428.
Botta-Orfila, T., et al., 2012. Age at onset in LRRK2-associated PD is modified by SNCA variants. J. Mol. Neurosci.
Braak, H., et al., 2003. Staging of brain pathology related to sporadic Parkinson's disease. Neurobiol. Aging 24, 197–211.
Campbell, B.C., et al., 2000. Accumulation of insoluble alpha-synuclein in dementia with Lewy bodies. Neurobiol. Dis. 7, 192–200.
Campbell, B.C., et al., 2001. The solubility of alpha-synuclein in multiple system atrophy differs from that of dementia with Lewy bodies and Parkinson's disease. J. Neurochem. 76, 87–96.
Cookson, M.R., 2009. Alpha-synuclein and neuronal cell death. Mol. Neurodegener. 4, 9.
Cookson, M.R., et al., 2008. Genetic neuropathology of Parkinson's disease. Int. J. Clin. Exp. Pathol. 1, 217–231.
Cremades, N., et al., 2012. Direct observation of the interconversion of normal and toxic forms of alpha-synuclein. Cell 149, 1048–1059.
Daher, J.P., et al., 2012. Neurodegenerative phenotypes in an A53T alpha-synuclein transgenic mouse model are independent of LRRK2. Hum. Mol. Genet. 21, 2420–2431.
Devine, M.J., et al., 2011. Pathogenic LRRK2 mutations do not alter gene expression in cell model systems or human brain tissue. PLoS One 6, e22489.
Fujiwara, H., et al., 2002. Alpha-synuclein is phosphorylated in synucleinopathy lesions. Nat. Cell Biol. 4, 160–164.
Galvin, J.E., et al., 2000. Neurodegeneration with brain iron accumulation, type 1 is characterized by alpha-, beta-, and gamma-synuclein neuropathology. Am. J. Pathol. 157 (2), 361–368.
Gandhi, P.N., et al., 2008. The Roc domain of leucine-rich repeat kinase 2 is sufficient for interaction with microtubules. J. Neurosci. Res. 86, 1711–1720.
Gilks, W.P., et al., 2005. A common LRRK2 mutation in idiopathic Parkinson's disease. Lancet 365, 415–416.
Gomez, A., Ferrer, I., 2010. Involvement of the cerebral cortex in Parkinson disease linked with G2019S LRRK2 mutation without cognitive impairment. Acta Neuropathol. 120, 155–167.
Greggio, E., Cookson, M.R., 2009. Leucine-rich repeat kinase 2 mutations and Parkinson's disease: three questions. ASN Neuro 1.
Greggio, E., et al., 2006. Kinase activity is required for the toxic effects of mutant LRRK2/dardarin. Neurobiol. Dis. 23, 329–341.
Guerreiro, P.S., et al., 2012. LRRK2 interactions with alpha-synuclein in Parkinson's disease brains and in cell models. J. Mol. Med. 91, 513–522 (Berl).
Healy, D.G., et al., 2008. Phenotype, genotype, and worldwide genetic penetrance of LRRK2-associated Parkinson' disease: a case–control study. Lancet Neurol. 7, 583–590.
Herzig, M.C., et al., 2012. High LRRK2 levels fail to induce or exacerbate neuronal alpha-synucleinopathy in mouse brain. PLoS One 7, e36581.
Imai, Y., et al., 2008. Phosphorylation of 4E-BP by LRRK2 affects the maintenance of dopaminergic neurons in *Drosophila*. EMBO J. 27, 2432–2443.
Jaleel, M., et al., 2007. LRRK2 phosphorylates moesin at threonine-558: characterization of how Parkinson's disease mutants affect kinase activity. Biochem. J. 405, 307–317.
Johansen, K.K., et al., 2009. Metabolomic profiling in LRRK2-related Parkinson's disease. PLoS One 4, e7551.

Johansen, K.K., et al., 2011. Subclinical signs in LRRK2 mutation carriers. Parkinsonism Relat. Disord. 17, 528–532.
Kingsbury, A.E., et al., 2010. Brain stem pathology in Parkinson's disease: an evaluation of the Braak staging model. Mov. Disord. 25, 2508–2515.
Kondo, K., et al., 2011. Alpha-synuclein aggregation and transmission are enhanced by leucine-rich repeat kinase 2 in human neuroblastoma SH-SY5Y cells. Biol. Pharm. Bull. 34, 1078–1083.
Lee, C.R., Tepper, J.M., 2009. Basal ganglia control of substantia nigra dopaminergic neurons. J. Neural Transm. Suppl. 71–90.
Li, J.Y., et al., 2008. Lewy bodies in grafted neurons in subjects with Parkinson's disease suggest host-to-graft disease propagation. Nat. Med. 14, 501–503.
Lin, X., et al., 2009. Leucine-rich repeat kinase 2 regulates the progression of neuropathology induced by Parkinson's-disease-related mutant alpha-synuclein. Neuron 64, 807–827.
Martin, I., et al., 2010. The impact of genetic research on our understanding of Parkinson's disease. Prog. Brain Res. 183, 21–41.
Mata, I.F., et al., 2006. LRRK2 in Parkinson's disease: protein domains and functional insights. Trends Neurosci. 29, 286–293.
McKeith, I.G., et al., 2005. Diagnosis and management of dementia with Lewy bodies: third report of the DLB Consortium. Neurology 65, 1863–1872.
Miller, D.W., et al., 2004. Alpha-synuclein in blood and brain from familial Parkinson disease with SNCA locus triplication. Neurology 62, 1835–1838.
Muntane, G., et al., 2008. Phosphorylation of tau and alpha-synuclein in synaptic-enriched fractions of the frontal cortex in Alzheimer's disease, and in Parkinson's disease and related alpha-synucleinopathies. Neuroscience 152, 913–923.
Nalls, M.A., et al., 2011. Imputation of sequence variants for identification of genetic risks for Parkinson's disease: a meta-analysis of genome-wide association studies. Lancet 377, 641–649.
Neumann, M., et al., 2002. Misfolded proteinase K-resistant hyperphosphorylated alpha-synuclein in aged transgenic mice with locomotor deterioration and in human alpha-synucleinopathies. J. Clin. Invest. 110, 1429–1439.
Paisan-Ruiz, C., et al., 2004. Cloning of the gene containing mutations that cause PARK8-linked Parkinson's disease. Neuron 44, 595–600.
Pchelina, S.N., et al., 2011. Reduced content of alpha-synuclein in peripheral blood leukocytes of patients with LRRK2-associated Parkinson's disease. Bull. Exp. Biol. Med. 150, 679–681.
Poulopoulos, M., et al., 2012. Clinical and pathological characteristics of LRRK2 G2019S patients with PD. J. Mol. Neurosci. 47, 139–143.
Qing, H., et al., 2009. Lrrk2 phosphorylates alpha synuclein at serine 129: Parkinson disease implications. Biochem. Biophys. Res. Commun. 387, 149–152.
Ross, O.A., et al., 2011. Association of LRRK2 exonic variants with susceptibility to Parkinson's disease: a case–control study. Lancet Neurol. 10, 898–908.
Sancho, R.M., et al., 2009. Mutations in the LRRK2 Roc-COR tandem domain link Parkinson's disease to Wnt signalling pathways. Hum. Mol. Genet. 18, 3955–3968.
Schulz-Schaeffer, W.J., 2010. The synaptic pathology of alpha-synuclein aggregation in dementia with Lewy bodies, Parkinson's disease and Parkinson's disease dementia. Acta Neuropathol. 120, 131–143.
Sharma, S., et al., 2011. LRRK2 expression in idiopathic and G2019S positive Parkinson's disease subjects: a morphological and quantitative study. Neuropathol. Appl. Neurobiol. 37, 777–790.
Smith, W.W., et al., 2005. Leucine-rich repeat kinase 2 (LRRK2) interacts with parkin, and mutant LRRK2 induces neuronal degeneration. Proc. Natl. Acad. Sci. U. S. A. 102, 18676–18681.
Smith, W.W., et al., 2006. Kinase activity of mutant LRRK2 mediates neuronal toxicity. Nat. Neurosci. 9, 1231–1233.
Spillantini, M.G., et al., 1997. Alpha-synuclein in Lewy bodies. Nature 388, 839–840.
Stafa, K., et al., 2012. GTPase activity and neuronal toxicity of Parkinson's disease-associated LRRK2 is regulated by ArfGAP1. PLoS Genet. 8, e1002526.
Tan, E.K., Skipper, L.M., 2007. Pathogenic mutations in Parkinson disease. Hum. Mutat. 28, 641–653.
Tong, Y., et al., 2009. R1441C mutation in LRRK2 impairs dopaminergic neurotransmission in mice. Proc. Natl. Acad. Sci. U. S. A. 106, 14622–14627.
Trancikova, A., et al., 2012. Phosphorylation of 4E-BP1 in the mammalian brain is not altered by LRRK2 expression or pathogenic mutations. PLoS One 7, e47784.
Vekrellis, K., et al., 2011. Pathological roles of alpha-synuclein in neurological disorders. Lancet Neurol. 10, 1015–1025.
Wakamatsu, M., et al., 2007. Accumulation of phosphorylated alpha-synuclein in dopaminergic neurons of transgenic mice that express human alpha-synuclein. J. Neurosci. Res. 85, 1819–1825.
West, A.B., et al., 2005. Parkinson's disease-associated mutations in leucine-rich repeat kinase 2 augment kinase activity. Proc. Natl. Acad. Sci. U. S. A. 102, 16842–16847.
Westerlund, M., et al., 2008. Lrrk2 and alpha-synuclein are co-regulated in rodent striatum. Mol. Cell. Neurosci. 39, 586–591.
Wider, C., et al., 2010. Leucine-rich repeat kinase 2 gene-associated disease: redefining genotype-phenotype correlation. Neurodegener. Dis. 7, 175–179.
Zhou, J., et al., 2011. Changes in the solubility and phosphorylation of alpha-synuclein over the course of Parkinson's disease. Acta Neuropathol. 121, 695–704.
Zimprich, A., et al., 2004. Mutations in LRRK2 cause autosomal-dominant parkinsonism with pleomorphic pathology. Neuron 44, 601–607.